Adaptive Sampling Algorithm for Macromodeling of Parameterized S-Parameter Responses

Dirk Deschrijver, *Member, IEEE*, Karel Crombecq, Huu Minh Nguyen, and Tom Dhaene, *Senior Member, IEEE*

***Abstract*—This paper presents a new adaptive sampling strategy for the parametric macromodeling of S-parameter-based frequency responses. It can be linked directly with the simulator to determine up front a sparse set of data samples that characterize the design space. This approach limits the overall simulation and macromodeling time. The resulting sample distribution can be fed into any kind of macromodeling technique, provided that it can deal with scattered data. The effectiveness of the approach is illustrated by a parameterized H-shaped microwave example.**

***Index Terms*—Adaptive sampling, frequency response, multivariate model, parametric macromodel, sequential design.**

I. Introduction

PARAMETRIC macromodels are important for the design, study, and optimization of microwave structures. Such macromodels approximate the S-parameter response of high-speed multiport systems as a function of frequency, and several layout variables that describe physical properties of the structure. They are frequently used for real-time design space exploration, design optimization, and sensitivity analysis.

The calculation of parametric macromodels has received a lot of attention over the past years, and many new modeling approaches were introduced. Most of them are either based on artificial neural network modeling [1], the multivariate Cauchy method [2], Thiele-type interpolation [3], combined rational-multinomial modeling [4], Kriging [5], radial basis functions [6], vector-fitting-based approaches [7]–[11], and others.

In order to simulate all data samples needed to build such a parametric macromodel, many full-wave analyses must be performed. Quite often, the data is collected over a predefined dense grid in the design space. However, since the number of data samples grows exponentially with the number of dimensions, an excessive amount of computer resources may be required. For this purpose, adaptive sampling strategies can be used to determine a quasi-minimal distribution of data samples that characterizes the overall system response [4].

Adaptive sampling strategies often select data samples in a sequential way by comparing intermediate macromodels. A drawback of this approach is that the selection of new data samples is highly dependent on the quality of these intermediate models. If their accuracy is degraded, e.g., by choosing a wrong model order or by spurious poles occuring in the design space, then the optimality of the sampling algorithm will break down. It is also noted that the selection of samples is affected by the model type (e.g., polynomial, rational, radial basis functions, etc.), which is not a desirable property. Moreover, it is found that many intermediate macromodels must be calculated before a suitable data distribution is obtained, leading to an overall slow and cost-ineffective procedure.

This paper presents a new generic sampling strategy that is able to resolve all these issues [12]. It can be linked directly with the simulator to adaptively select a representative set of data samples before any kind of macromodeling procedure is applied. The resulting distribution of the data can be fed into an arbitrary macromodeling technique, provided that it can deal with scattered data. The effectiveness of the approach is illustrated by a scalable microwave H-antenna example.

II. Preliminaries and Notation

Parametric macromodeling algorithms compute a multivariate model from a set of parameterized S-parameter *data samples* $\{(s, \boldsymbol{g}), H(s, \boldsymbol{g})\}$. These S-parameters $H(s, \boldsymbol{g}) \in \mathbb{C}$ depend on the frequency $s = j\omega \in j\mathbb{R}$ and several design parameters $\boldsymbol{g} = \left\{g^{(n)}\right\}_{n=1}^{N} \subset \mathbb{R}^N$. These design parameters are the layout and material parameters, which describe, e.g., the metallizations of a component (lengths, widths, etc.) or its substrate parameters (thickness, dielectric constant, losses, etc.).

A full-wave electromagnetic (EM) simulator is used to simulate the data samples over a fixed set of T discrete frequencies $\{s_t\}_{t=1}^{T}$ at scattered locations in the design space. The *design space* is defined as a subspace of $\mathbb{R}^N$ that is bounded by the parameter ranges of $\boldsymbol{g}$, while the scattered locations are instances of the design parameters. In this paper, these instances are called *data points*. To limit the overall simulation cost, an adaptive sampling algorithm is introduced to select a limited set of data points $P = \{\boldsymbol{p}_k\}_{k=1}^{K}$ in an intelligent way. Note that each data point $\boldsymbol{p}_k = \left(p_k^{(1)}, \ldots, p_k^{(N)}\right)$ contains scalar values that correspond to the design parameters $\boldsymbol{g}$. The goal of the adaptive sampling algorithm is to minimize the number of selected data points, while maximizing the model accuracy.

Manuscript received January 26, 2010; revised July 09, 2010; accepted August 24, 2010. Date of publication November 18, 2010; date of current version January 12, 2011. This work was supported by the Research Foundation Flanders. The work of D. Deschrijver and K. Crombecq was supported under an FWO Fellowship.

D. Deschrijver, H. M. Nguyen, and T. Dhaene are with the Department of Information Technology, Ghent University–IBBT, 9000 Ghent, Belgium (e-mail: dirk.deschrijver@intec.ugent.be; huuminh.nguyen@intec.ugent.be; tom.dhaene@intec.ugent.be).

K. Crombecq is with the Department of Mathematics and Computer Science, University of Antwerp, 2020 Antwerp, Belgium (e-mail: karel.crombecq@ua.ac.be).

Color versions of one or more of the figures in this paper are available online at http://ieeexplore.ieee.org.

Digital Object Identifier 10.1109/TMTT.2010.2090407

III. Methodology of Adaptive Algorithm

The adaptive algorithm selects a reduced set of data points that is used to characterize the overall behavior of the response. To obtain a robust procedure, a tradeoff between two important criteria must be made: *exploration* and *exploitation*.

- Exploration is the act of exploring the design space in order to find key regions that have not yet been identified before. Note that exploration does not involve the response of the system, but only the location of the data points and the way they are distributed over the design space. It ensures that the design space is filled up with data points that are spread as evenly as possible.
- Exploitation means that data points are selected in regions of the design space that are identified as potentially interesting. It is clear that regions where the response is highly dynamic require a finer sampling density than regions where the response shows little or no variation.

The new sampling algorithm is a generic approach that combines both criteria in a balanced way [13], [14]. It starts from a small number of initial data points so that the majority of data points can be chosen adaptively. For the exploration criterion, the density of data points is quantified by computing a Voronoi tessellation of the data points and by calculating the volume of each Voronoi cell (Section IV). For the exploitation criterion, the dynamic variation of the response is quantified by computing simple local linear approximation models that are compared with the true system response (Section V). Both criteria are translated into a combined metric function that is used to rank the neighborhood of the data points. Based on this ranking, the undersampled regions of the design space are identified and the optimal location for additional data points is derived (Section VI). This procedure of adding data points is repeated sequentially until the algorithm is terminated.

IV. Exploration—Voronoi Tessellations

The density of data points is assessed by computing a Voronoi tessellation [15] of the design space and by estimating the volume of each cell. Cells having a large volume correspond to regions in the design space that are sampled sparsely.

Let us assume that a discrete and pairwise distinct set of points $P = \{\boldsymbol{p}_k\}_{k=1}^{K}$ in the design space is given. The dominance of a point $\boldsymbol{p}_k$ over $\boldsymbol{p}_m$ is then defined as follows:

$$\mathrm{dom}(\boldsymbol{p}_k,\boldsymbol{p}_m) = \left\{\boldsymbol{p}\in\mathbb{R}^N \,|\, \|\boldsymbol{p}-\boldsymbol{p}_k\| \le \|\boldsymbol{p}-\boldsymbol{p}_m\|\right\}. \quad (1)$$

It represents a closed half-plane that is bounded by the perpendicular bisector of $\boldsymbol{p}_k$ and $\boldsymbol{p}_m$, and separates all points that lie closer to $\boldsymbol{p}_k$ than $\boldsymbol{p}_m$. The Voronoi cell C_k of $\boldsymbol{p}_k$ determines the portion of the design space that lies in all the dominances of $\boldsymbol{p}_k$ over all other data points in the set P

$$C_k = \bigcap_{\boldsymbol{p}_m\in P\setminus\boldsymbol{p}_k} \mathrm{dom}(\boldsymbol{p}_k,\boldsymbol{p}_m). \quad (2)$$

It is clear that C_k contains all points in the design space lying closer to $\boldsymbol{p}_k$ than any other point in P. The complete set of cells $\{C_k\}_{k=1}^{K}$ tessellates the design space, and is called the Voronoi tessellation corresponding to the set P. Computing the Voronoi tessellation is usually done by calculating the Delaunay triangulation from which the Voronoi tessellation is obtained. In order to compute the volume of each Voronoi cell, the unbounded Voronoi cells near the border of the parameter ranges are bounded. The volume (Vol) of each cell can then easily be estimated by means of Monte Carlo methods [16].

To assess the density of the data points around $\boldsymbol{p}_k$, the following normalized metric $V(\boldsymbol{p}_k)\in[0,1]$ is introduced:

$$V(\boldsymbol{p}_k) = \frac{\mathrm{Vol}(C_k)}{\mathrm{Vol}(C_1)+\cdots+\mathrm{Vol}(C_K)}. \quad (3)$$

Note that $V(\boldsymbol{p}_k)$ quantifies the portion of the design space that is contained within each Voronoi cell C_k of $\boldsymbol{p}_k$.

V. Exploitation—Local Linear Approximations

Regions of the design space with a high dynamical behavior are identified as follows. For each point $\boldsymbol{p}_k$ in P, a suitable set of V neighboring points $N(\boldsymbol{p}_k)$ is chosen (Section V-A). For each frequency $\{s_t\}_{t=1}^{T}$, these neighbors are used to estimate the gradient $\nabla H(s_t,\boldsymbol{g})$ that characterizes the best local linear approximation $\tilde{H}(s_t,\boldsymbol{g})$ at $\boldsymbol{p}_k$ (Section V-B). The response of this approximation is compared to the true response $H(s_t,\boldsymbol{g})$ at the neighboring points $N(\boldsymbol{p}_k)$, and quantifies the dynamic variation in the region of $\boldsymbol{p}_k$. A large deviation indicates the regions where the data is varying more rapidly.

A. Selection of Neighboring Samples

To accurately estimate the gradient of the response at a certain point $\boldsymbol{p}_k$, a set of neighboring data points $N(\boldsymbol{p}_k)$

$$N(\boldsymbol{p}_k) = \{\boldsymbol{p}_{kv}\}_{v=1}^{V} \text{ with } N(\boldsymbol{p}_k)\subset P\setminus\{\boldsymbol{p}_k\} \quad (4)$$

must be selected that provide as much information as possible. This means that neighbors should cover each direction in the design space equally well. Therefore, neighbors should satisfy two important properties: *cohesion* and *adhesion*.

- Cohesion implies that they must lie as close to the point $\boldsymbol{p}_k$ as possible such that $C(N(\boldsymbol{p}_k))$ is minimized

$$C(N(\boldsymbol{p}_k)) = \frac{1}{V}\sum_{v=1}^{V}\|\boldsymbol{p}_{kv}-\boldsymbol{p}_k\|. \quad (5)$$

- Adhesion implies that they must lie as far away from each other as possible such that $A(N(\boldsymbol{p}_k))$ is maximized

$$A(N(\boldsymbol{p}_k)) = \frac{1}{V}\sum_{v=1}^{V}\min\{\|\boldsymbol{p}_{kv}-\boldsymbol{p}_{kw}\|, \forall\, w\neq v\}. \quad (6)$$

These two properties necessarily conflict with each other so a compromise must be made. In the case of $V = 2N$, it is proven in [17] that the optimal configuration is the N-dimensional cross-polytope configuration because it maximizes the adhesion (6) in all dimensions. Since $\sqrt{2}C(N(\boldsymbol{p}_k))$ is the upper bound for the adhesion value of any neighborhood with cohesion $C(N(\boldsymbol{p}_k))$, a cross-polytope ratio $R(N(\boldsymbol{p}_k))$ is defined,

which indicates how closely a neighborhood resembles a cross-polytope (It is assumed that $N > 1$.)

$$R(N(\boldsymbol{p}_k)) = \frac{A(N(\boldsymbol{p}_k))}{\sqrt{2}C(N(\boldsymbol{p}_k))}. \tag{7}$$

If $R(N(\boldsymbol{p}_k)) = 1$, then the neighborhood forms a perfect cross-polytope configuration. Also, if $R(N(\boldsymbol{p}_k)) = 0$, then all neighboring data points must lie in the exact same spot, reducing the adhesion to 0. Since the distance from $\boldsymbol{p}_k$ should also be taken into account, the cross-polytope ratio (7) is divided by the cohesion, leading to the neighborhood score

$$S(N(\boldsymbol{p}_k)) = \frac{R(N(\boldsymbol{p}_k))}{C(N(\boldsymbol{p}_k))}. \tag{8}$$

Note that neighboring data points $N(\boldsymbol{p}_k)$ are ideally chosen in such a way that the neighborhood score (8) is maximized.

B. Gradient and Local Linear Approximation

The gradient of the response $H(s_t, \boldsymbol{g})$ is defined as

$$\nabla H(s_t, \boldsymbol{g}) = \left(\frac{\partial H(s_t, \boldsymbol{g})}{\partial g^{(1)}}, \frac{\partial H(s_t, \boldsymbol{g})}{\partial g^{(2)}}, \ldots, \frac{\partial H(s_t, \boldsymbol{g})}{\partial g^{(N)}} \right). \tag{9}$$

It is used to characterize the best local linear approximation for $\tilde{H}(s_t, \boldsymbol{g})$ around a specified point $\boldsymbol{p}_k$ as follows [18]:

$$\tilde{H}(s_t, \boldsymbol{g}) = H(s_t, \boldsymbol{p}_k) + \nabla H(s_t, \boldsymbol{g})|_{p_k} (\boldsymbol{g} - \boldsymbol{p}_k). \tag{10}$$

Note that $\nabla H(s_t, \boldsymbol{g})|_{pk} = A^{-1}b$ is estimated by fitting a hyperplane through point $\boldsymbol{p}_k$ based on its V neighbors $\{\boldsymbol{p}_{kv}\}_{v=1}^{V}$

$$A = \begin{bmatrix} p_{k1}^{(1)} - p_k^{(1)} & p_{k1}^{(2)} - p_k^{(2)} & \ldots & p_{k1}^{(N)} - p_k^{(N)} \\ p_{k2}^{(1)} - p_k^{(1)} & p_{k2}^{(2)} - p_k^{(2)} & \ldots & p_{k2}^{(N)} - p_k^{(N)} \\ \ldots & \ldots & \ldots & \ldots \\ p_{kV}^{(1)} - p_k^{(1)} & p_{kV}^{(2)} - p_k^{(2)} & \ldots & p_{kV}^{(N)} - p_k^{(N)} \end{bmatrix} \tag{11}$$

$$b = \begin{bmatrix} H(s_t, \boldsymbol{p}_{k1}) & H(s_t, \boldsymbol{p}_{k2}) & \ldots & H(s_t, \boldsymbol{p}_{kV}) \end{bmatrix}^T. \tag{12}$$

Once the gradient is estimated, the dynamical behavior around point $\boldsymbol{p}_k$ is quantified by comparing the response of $\tilde{H}(s_t, \boldsymbol{g})$ with the true response $H(s_t, \boldsymbol{g})$ at the neighboring points $\boldsymbol{p}_{kv}$

$$\bar{E}(\boldsymbol{p}_k) = \max_t \left(\sum_{v=1}^{V} \left| \tilde{H}(s_t, \boldsymbol{p}_{kv}) - H(s_t, \boldsymbol{p}_{kv}) \right| \right). \tag{13}$$

To obtain a normalized metric $E(\boldsymbol{p}_k) \in [0, 1]$, one defines

$$E(\boldsymbol{p}_k) = \frac{\bar{E}(\boldsymbol{p}_k)}{\bar{E}(\boldsymbol{p}_1) + \cdots + \bar{E}(\boldsymbol{p}_K)}. \tag{14}$$

The metric $E(\boldsymbol{p}_k)$ quantifies the portion of the dynamic variation in the response that is located near point $\boldsymbol{p}_k$.

VI. Additional Data Point Selection

The exploration-based metric $V(\boldsymbol{p}_k)$ in (3) quantifies data points according to the size of their corresponding Voronoi cell, while the exploitation-based metric $E(\boldsymbol{p}_k)$ in (14) quantifies data points according to the local variation of the response. Both are combined into a global metric that is used for ranking

$$G(\boldsymbol{p}_k) = (1 + V(\boldsymbol{p}_k))(1 + E(\boldsymbol{p}_k)). \tag{15}$$

Data points associated with large values of (15) are located in regions that are likely undersampled, whereas the smaller values of (15) correspond to regions that are sampled sufficiently dense. If the data point with the maximum value of (15) is denoted by $\boldsymbol{p}_m$, then the algorithm select an additional data point inside the Voronoi cell C_m. Its exact location is chosen in such a way that the distance from the neighbors $N(\boldsymbol{p}_m)$ is maximized. Once the new data point is added to P, the procedure is repeated until the algorithm is terminated.

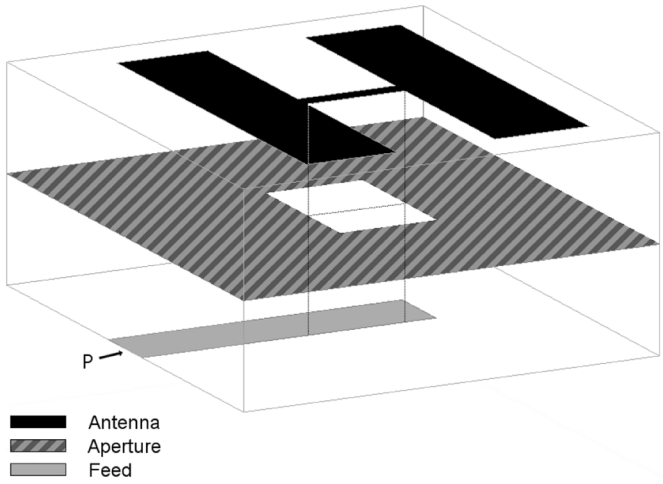

Fig. 1. 3-D view of the microwave H-antenna.

VII. Example: Microwave H-Antenna

This example deals with the parametric macromodeling of the reflection coefficient S_{11} of a scalable H-shaped microwave antenna. Fig. 1 shows a 3-D view of the antenna, which consists of three layers: a top layer with the H-shaped antenna, a bottom layer with the feed line, and a middle slot layer with a rectangular aperture that realizes the coupling between the feed and the antenna. Fig. 2 shows a top view of the three metal layers along with their respective dimensions. A cross section of the structure is shown in Fig. 3, depicting the vertical position of the metal layers in the dielectric. The design parameters of the model are the length L of the antenna and the width W of the aperture. The frequency range of interest varies between $f \in [4.5 - 5.5\ \text{GHz}]$. All data samples are simulated with the full-wave planar EM simulator ADS Momentum [19], and the data points in the design space are selected by the proposed adaptive sampling algorithm.

A. Adaptive Sample Selection

As a first example, the parameter ranges of the model are set to $L \in [3 - 11\ \text{mm}]$ and $W \in [0.01 - 6\ \text{mm}]$. The algorithm starts by simulating an initial set of 24 data points, as shown

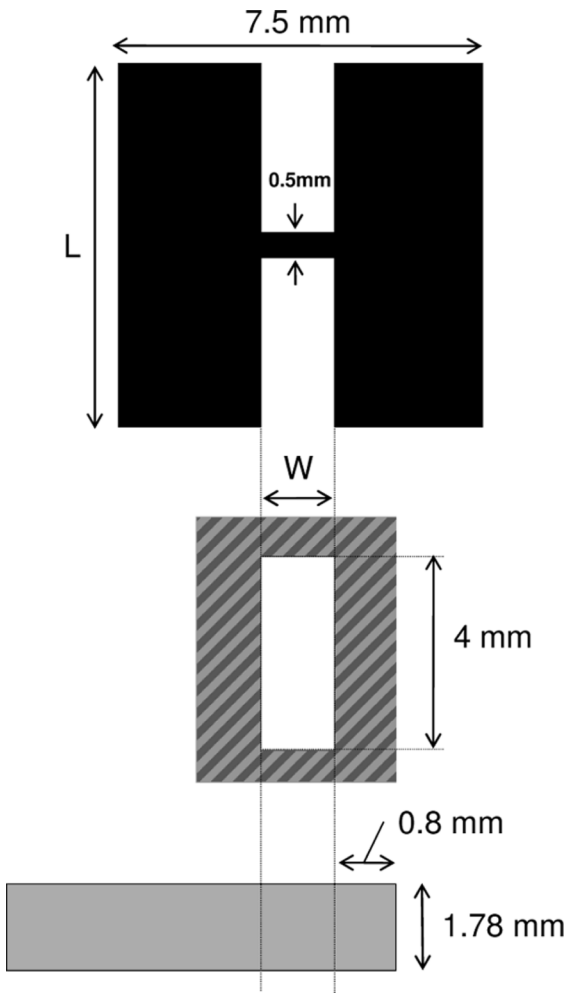

Fig. 2. Top view of the microwave H-antenna.

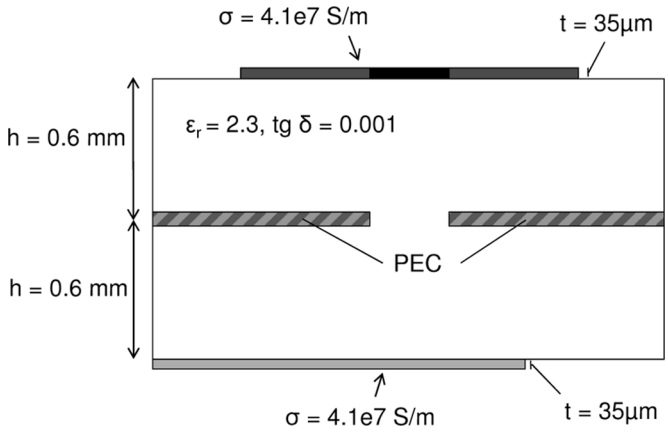

Fig. 3. Cross section of the microwave H-antenna.

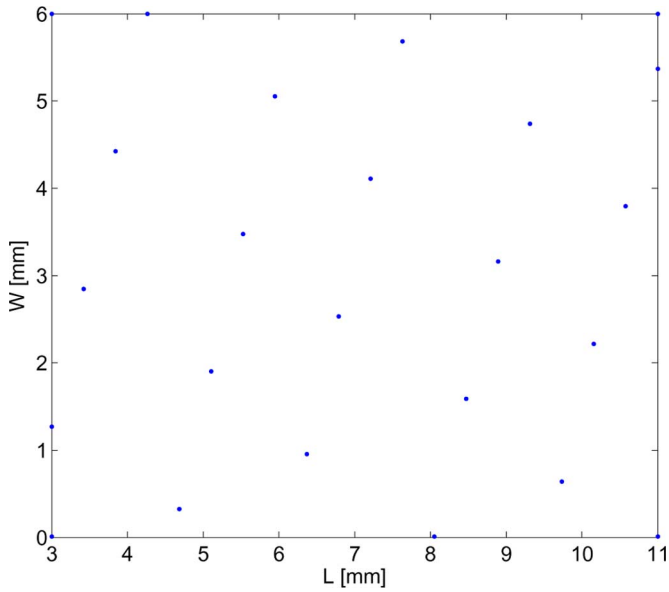

Fig. 4. Adaptive sampling of 24 scattered data points (dots).

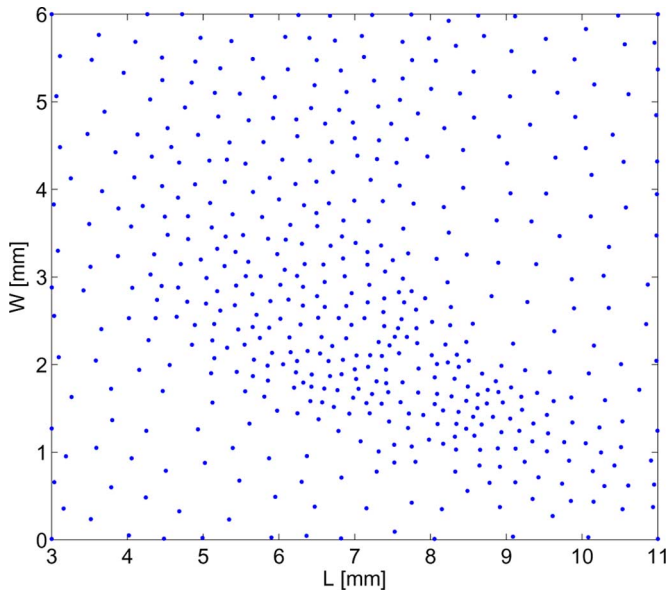

Fig. 5. Adaptive sampling of 500 scattered data points (dots).

in Fig. 4. This set consists of four data points that are located at the corners of the design space and 20 additional data points that are scattered in the design space. Based on the combined metric function (15), the neighborhood of each data point is ranked, and the undersampled regions of the design space are identified. In successive iteration steps, additional data points are selected. Figs. 5–7 show the distribution of 500, 1000, and 2000 data points that are chosen by the algorithm, respectively. It is seen that the overall design space is well resolved, and that the data points are spread in an adaptive nonuniform way.

To validate the effectiveness of the sample distribution, the parametrized frequency response is simulated for a constant value of $W = 2.406$ mm and a varying length L. In terms of the design space, this corresponds to the horizontal solid line (red in online version) that is shown in Fig. 7. It is seen from this figure that data points are distributed more densely if L has a value in between approximately 5 and 8 mm, as marked by the vertical dashed lines (black). The reason becomes clear when Fig. 8 is considered. If L is varied in between these values, the frequency response contains a sharp resonance that moves toward the lower frequencies as the length increases. For other values

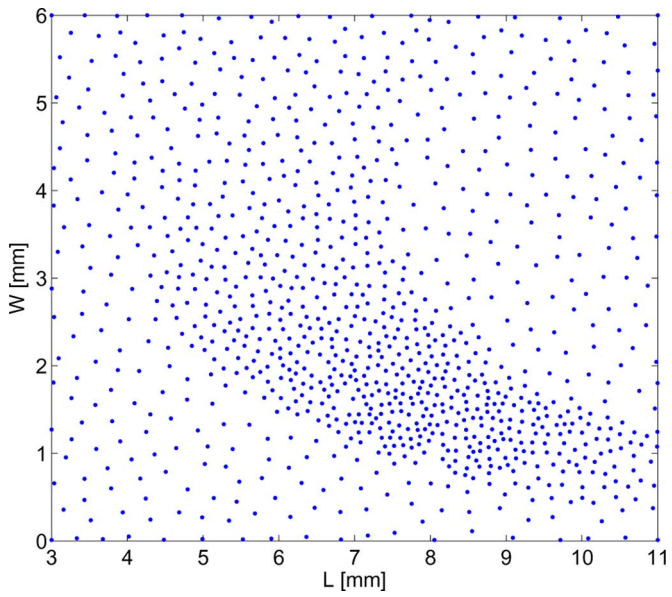

Fig. 6. Adaptive sampling of 1000 scattered data points (dots).

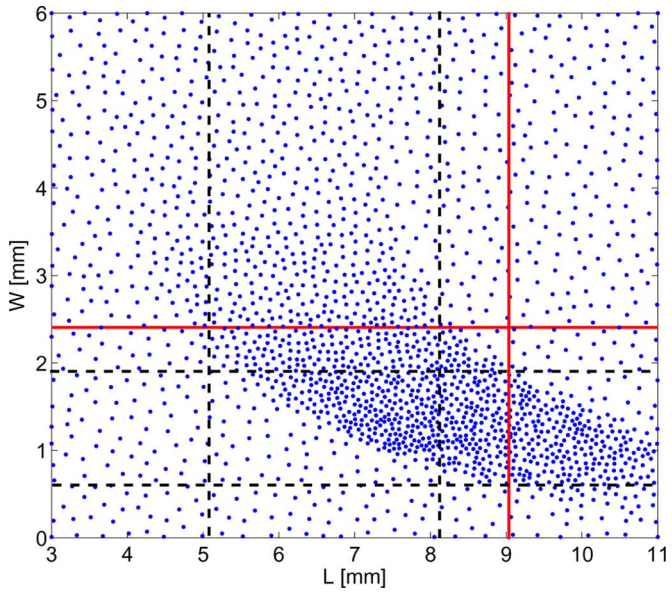

Fig. 7. Adaptive sampling of 2000 scattered data points (dots).

of L, this resonance is located outside the frequency range of interest, leading to a smoother frequency response.

As an additional test, the frequency response is simulated for a constant value of $L = 9$ mm and a varying width W. This corresponds to the vertical solid line (red in online version) shown in Fig. 7. Here, it is also found that the data points are distributed more densely if W has a value in between approximately 0.7 and 1.9 mm, as marked by the horizontal dashed lines (black). In between these values, the frequency response contains a sharp resonance that moves towards the lower frequencies as the width increases, as shown in Fig. 9. For other values of W, this resonance is located outside the frequency range.

These results confirm that the dynamical regions of the design space are indeed sampled more densely than other regions where the frequency response shows less variation.

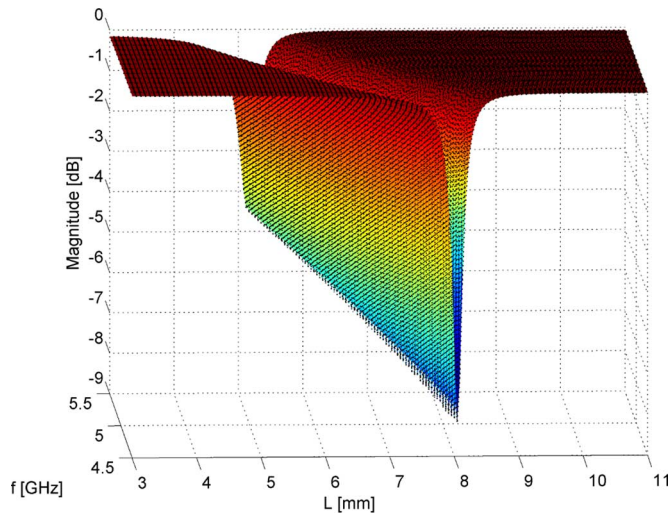

Fig. 8. Magnitude parameterized S-parameter response for $W = 2.406$ mm.

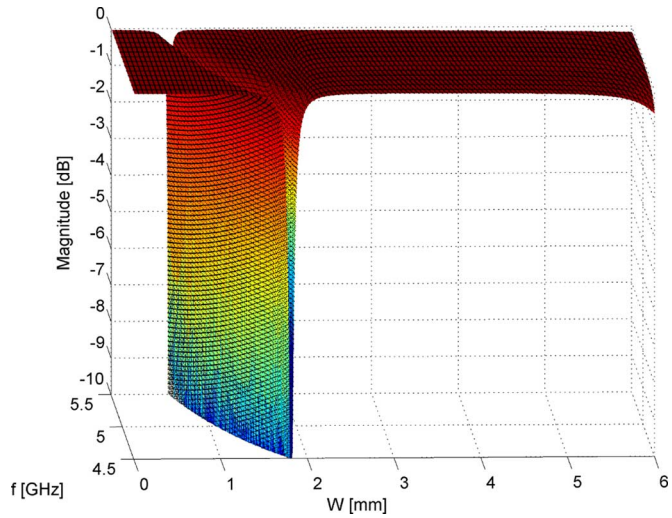

Fig. 9. Magnitude parameterized S-parameter response for $L = 9$ mm.

B. Parametric Macromodeling

As a second example, the parametric modeling of the same H-shaped antenna is considered. In this case, the parameter ranges of the macromodel are set to $L \in [6 - 7.1 \text{ mm}]$ and $W \in [1.01 - 1.1 \text{ mm}]$, and the proposed algorithm is applied to compute a representative set of 225 data points that are scattered over the design space. The distribution of the data points is shown in Fig. 10, and it is observed that data points are sampled more densely in the upper right corner. This area corresponds to the region of the design space where the resonance moves into the upper part of the frequency range from outside, as the value of L increases. A closer inspection of Figs. 7 and 10 reveals that a similar distribution of the data points is chosen. As a comparison, the same number of data points are simulated over a classical predefined sampling that does not take the dynamical behavior of the response into account, e.g., a uniform 15×15 grid, as shown in Fig. 11.

To compute a parametric macromodel from the simulated data samples, any kind of modeling technique can be applied. In this case, the modeling approach in [20] is adopted because

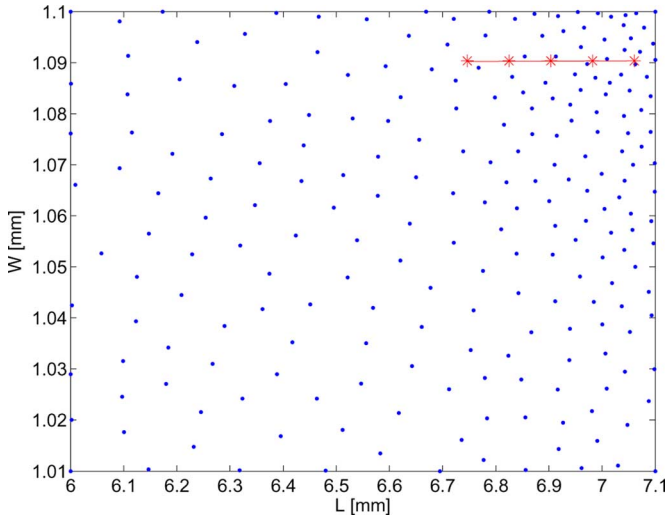

Fig. 10. Adaptive sampling of 225 scattered data points (dots).

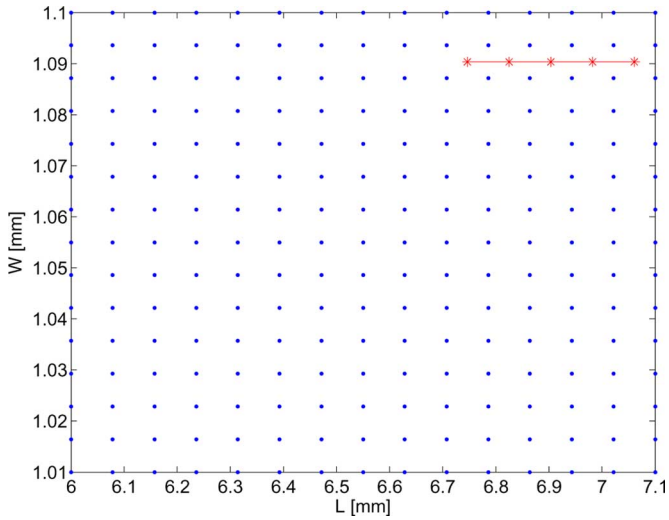

Fig. 11. Uniform sampling of 225 grid-based data points (dots).

it can deal with scattered data and offers the possibility to enforce stability and passivity by construction. First, the selected data points of the adaptive algorithm are used to build a triangulation of the design space. Some linear interpolation inside a simplex is then performed to evaluate the model at intermediate data points. It is noted that this interpolation scheme is local, and therefore, highly sensitive to the distribution and the density of the selected data points.

In order to assess the importance of the sampling, some parametric macromodels are computed based on the adaptive sampling (shown in Fig. 10) and the uniform sampling (shown in Fig. 11). The response of both parametric macromodels is evaluated for some arbitrary data points that are located in the most dynamic region of the design space, and the response of these models is compared to the simulation data. These data points are marked by five red asterisks (in online version) in both figures.

Table I shows a comparison of the maximum absolute error over all frequencies f in each of these data points. It is clear that the accuracy in the adaptive case is indeed better than the

TABLE I
COMPARISON OF MAXIMUM ABSOLUTE ERROR

Width W	Length L	Uniform	Adaptive
1.0903 mm	6.7464 mm	-60.16 dB	-73.32 dB
1.0903 mm	6.8250 mm	-56.78 dB	-64.07 dB
1.0903 mm	6.9035 mm	-54.04 dB	-75.62 dB
1.0903 mm	6.9821 mm	-59.67 dB	-66.25 dB
1.0903 mm	7.0607 mm	-53.83 dB	-88.69 dB

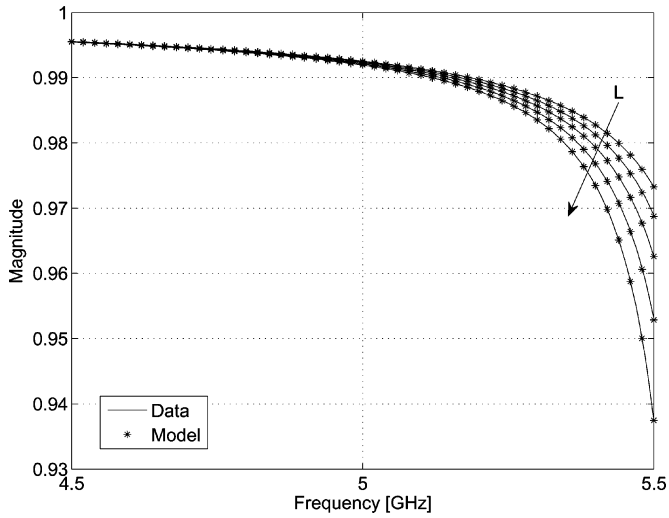

Fig. 12. Magnitude adaptive macromodel and reference data for varying L.

accuracy in the uniform case. This follows from the fact that the data points are sampled more densely in the regions where the frequency response is varying more rapidly. As a final illustration, the response of the adaptive macromodel is compared to the simulated frequency response in Fig. 12, and it shows that an excellent agreement is observed.

VIII. DISCUSSION

In many practical cases, it is possible to characterize the entire frequency response at a limited (or no) additional cost, when compared to the simulation of a single frequency sample. In the frequency domain, standard commercial simulation tools can calculate the entire frequency sweep by simulating the system at a limited number of frequencies (e.g., using AFS algorithms [21]). Also in the time domain, an entire sweep of frequency samples is calculated by applying a fast Fourier transform (FFT) to the impulse response. Therefore, the adaptive sampling algorithm treats frequency as a separate variable. Note, however, that it is possible to include the frequency as a regular design parameter, by making some minor modifications to the algorithm, particularly in (13).

IX. CONCLUSIONS

In order to limit the overall simulation and macromodeling time, an efficient adaptive sampling algorithm is proposed for parametric macromodeling of S-parameter-based system responses. It can easily be linked to any full-wave EM simulator to select a representative set of scattered data points in a sequential way. Note that the sampling algorithm does not

depend on the multivariate macromodeling technique used. The benefits of the approach are illustrated by an example.

REFERENCES

[1] A. H. Zaabab, Q. J. Zhang, and M. Nakhla, "A neural network modeling approach to circuit optimization and statistical design," *IEEE Trans. Microw. Theory Tech.*, vol. 43, no. 6, pp. 1349–1558, Jun. 1995.

[2] A. Lamecki, P. Kozakowski, and M. Mrozowski, "Efficient implementation of the Cauchy method for automated CAD-model construction," *IEEE Microw. Wireless Compon. Lett.*, vol. 13, no. 7, pp. 268–270, Jul. 2003.

[3] R. Lehmensiek and P. Meyer, "Creating accurate multivariate rational interpolation models for microwave circuits by using efficient adaptive sampling to minimize the number of computational electromagnetic analyses," *IEEE Trans. Microw. Theory Tech.*, vol. 49, no. 8, pp. 1419–1419, Aug. 2001.

[4] J. De Geest, T. Dhaene, N. Faché, and D. De Zutter, "Adaptive CAD-model building algorithm for general planar microwave structures," *IEEE Trans. Microw. Theory Tech.*, vol. 47, no. 9, pp. 1801–1809, Sep. 1999.

[5] J. P. C. Kleijnen and W. C. M. Van Beers, "Application driven sequential designs for simulation experiments: Kriging metamodels," *J. Operat. Res. Soc.*, vol. 55, pp. 876–883, Dec. 2004.

[6] A. Lamecki, P. Kozakowski, and M. Mrozowski, "CAD-model construction based on adaptive radial basis functions interpolation technique," in *15th Int. Microw., Radar, Wireless Commun. Conf.*, May 2004, vol. 3, pp. 799–802.

[7] B. Gustavsen and A. Semlyen, "Rational approximation of frequency domain responses by vector fitting," *IEEE Trans. Power Del.*, vol. 14, no. 3, pp. 1052–1061, Jul. 1999.

[8] D. Deschrijver, T. Dhaene, and D. De Zutter, "Robust parametric macromodeling using multivariate orthonormal vector fitting," *IEEE Trans. Microw. Theory Tech.*, vol. 56, no. 7, pp. 1661–1667, Jul. 2008.

[9] D. Deschrijver and T. Dhaene, "Stability and passivity enforcement of parametric macromodels in time and frequency domain," *IEEE Trans. Microw. Theory Tech.*, vol. 56, no. 11, pp. 2435–2441, Nov. 2008.

[10] T. Dhaene and D. Deschrijver, "Stable parametric macromodeling using a recursive implementation of the vector fitting algorithm," *IEEE Microw. Wireless Compon. Lett.*, vol. 19, no. 2, pp. 415–420, Feb. 2009.

[11] P. Triverio, S. Grivet-Talocia, and M. S. Nakhla, "A parameterized macromodeling strategy with uniform stability test," *IEEE Trans. Adv. Packag.*, vol. 32, no. 1, pp. 205–215, Feb. 2009.

[12] K. Crombecq, I. Couckuyt, D. Gorissen, and T. Dhaene, "A novel sequential design strategy for global surrogate modeling," in *Proc. 41th Winter Simulation Conf.*, Dec. 2009, accepted for publication.

[13] D. C. Montgomery, *Design and Analysis of Experiments*, 5th ed. New York: Wiley, 2000.

[14] A. Forrester, A. Sobester, and A. Keane, *Engineering Design via Surrogate Modelling: A Practical Guide*. New York: Wiley, 2008.

[15] F. Aurenhammer, "Voronoi diagrams—A survey of a fundamental geometric data structure," *ACM Comput. Surveys*, vol. 23, no. 3, pp. 345–405, 1991.

[16] N. Metropolis and S. Ulam, "The Monte Carlo method," *J. Amer. Statist. Assoc.*, vol. 44, no. 247, pp. 335–341, 1949.

[17] H. Cohn and A. Kumar, "Universally optimal distribution of points of spheres," *J. Amer. Math. Soc.*, vol. 21, no. 1, pp. 99–148, Jan. 2007.

[18] T. Hachisuka, W. Jarosz, R. P. Weistroffer, K. Dale, G. Humphreys, M. Zwicker, and H. W. Jensen, "Multidimensional adaptive sampling and reconstruction for ray tracing," *ACM Trans. Graphics*, vol. 27, no. 3, p. 10, 2008.

[19] Agilent EEsof COMMS EDA,ADS Momentum Software. Agilent Technol. Inc., Santa Rosa, CA, 2009.

[20] F. Ferranti, T. Dhaene, and L. Knockaert, "Passivity-preserving interpolation-based parameterized macromodeling of scattered data," *IEEE Microw. Wireless Compon. Lett.*, vol. 20, no. 3, pp. 133–135, Mar. 2010.

[21] T. Dhaene, J. Ureel, N. Faché, and D. De Zutter, "Adaptive frequency sampling algorithm for fast and accurate S-parameter modeling of general planar structures," in *IEEE MTT-S Int. Microw. Symp. Dig.*, Orlando, FL, May 1995, vol. 3, pp. 1427–1430.

Dirk Deschrijver (M'09) was born in Tielt, Belgium, on September 26, 1981. He received the Master degree (licentiaat) and Ph.D. degree in computer science from the University of Antwerp, Antwerp, Belgium, in 2003 and 2007, respectively.

From May to October 2005, he was a Marie Curie Fellow with the Scientific Computing Goup, Eindhoven University of Technology, Eindhoven, The Netherlands. He is currently an FWO Post-Doctoral Research Fellow with the Department of Information Technology (INTEC), Ghent University, Ghent, Belgium. His research interests include robust parametric macromodeling, rational least-squares approximation, orthonormal rational functions, system identification and broadband macromodeling techniques.

Karel Crombecq was born in Antwerp, Belgium, on November 6, 1984. He received the Master's degree in computer science from the University of Antwerp, Antwerp, Belgium in 2006, and is currently working toward the Ph.D. degree at the University of Antwerp.

He is currently with the CoMP Research Group, Department of Computer Science and Mathematics, University of Antwerp. His research interests include distributed surrogate modeling, adaptive sampling techniques, and machine learning.

Huu Minh Nguyen was born in Hanoi, Vietnam, on June 13, 1985. He received the Erasmus Mundus M.Sc. degree in photonics from Ghent University, Ghent, Belgium, in 2008, and is currently working toward the Ph.D. degree in information technology at Ghent University.

Since April 2009, he has been with the Department of Information Technology (INTEC), Ghent University. His research interests include supervised machine learning, bioinformatics, and multivariate regression or classification problems.

Tom Dhaene (M'94–SM'05) was born in Deinze, Belgium, on June 25, 1966. He received the Ph.D. degree in electrotechnical engineering from the University of Ghent, Ghent, Belgium, in 1993.

From 1989 to 1993, he was a Research Assistant with the Department of Information Technology, University of Ghent, where his research was focused on different aspects of full-wave EM circuit modeling, transient simulation, and time-domain characterization of high-frequency and high-speed interconnections. In 1993, he joined the EDA company Alphabit (now part of Agilent). He was one of the key developers of the planar EM simulator ADS Momentum. Since September 2000, he has been a Professor with the Department of Mathematics and Computer Science, University of Antwerp, Antwerp, Belgium. Since October 2007, he has been a Full Professor with the Department of Information Technology (INTEC), Ghent University, Ghent, Belgium. He has authored or coauthored, or has contributed to over 220 peer-reviewed papers and abstracts in international conference proceedings, journals, and books.